

Electronic Supporting Information (ESI)

Electret-induced Electric Field Assisted Luminescence Modulation for Interactive Visualized Sensing in a Non-contact Mode

Hai Lu Wang^{‡ac}, Li Su^{‡b}, Hua Yang Li^d, Zhong Lin Wang^f, Guang Zhu^{acde*}

^a. CAS Centre for Excellence in Nanoscience, Beijing Key Laboratory of Micro-nano Energy and Sensor, Beijing Institute of Nanoenergy and Nanosystems, Chinese Academy of Sciences, Beijing 100083, P. R.

^b. Hebei Key Laboratory of Optic-Electronic Information and Materials, National-Local Joint Engineering Laboratory of New Energy Photoelectric Devices, College of Physics Science and Technology, Hebei University, Baoding, 071002, China.

^c. School of Nanoscience and Technology, University of Chinese Academy of Sciences, Beijing 100048, P. R. China

^d. New Materials Institute, Department of Mechanical, Materials and Manufacturing Engineering, University of Nottingham Ningbo China, Ningbo 315100, P. R. China

^e. Centre on Nanoenergy Research, School of Physical Science and Technology, Guangxi University, Nanning 530004, P. R. China.

^f. School of Materials Science and Engineering, Georgia Institute of Technology, Atlanta GA 30332, USA

[‡] These authors contributed equally to this work.

1. Experimental section

Fabrication of the non-contact interactive visualised sensor.

The NCIVS was fabricated through a corona-charging method. First, an electret film made of PTFE film was pasted on a substrate with the dimensions of $5 \times 5 \text{ cm}^2$. The PDMS matrix, PTFE nanoparticles and ZnS: Cu particles were mixed and stirred for homogeneous dispersion. Then, a curing agent for PDMS was added with a weight ratio of 1:10. Afterwards, the uncured composite was transferred to the surface of the PTFE film using the blade-coating method. Corona charging was conducted immediately after the coating, which continued for 10 min with needle distance of 5 cm and needle voltage of 7 kV. Finally, the sample was placed in the oven at $75 \text{ }^\circ\text{C}$ for 4 h for PDMS curing.

COMSOL Model Settings.

A two-dimensional model was used to analyse the static electric field distribution and the dynamic electric field variation of the NCIVS. The dimensions of the PTFE film were $20 \times 20 \times 1 \text{ mm}^3$, and the dimensions of the Cu film were $5 \times 5 \times 0.05 \text{ mm}^3$. The thickness of the luminescent layer was set at 0.5 mm. The distance between the Cu film and the NCIVS was 0.5 mm. The surface charge density on the PTFE and contact object were set as -0.49 mC/m^2 and $+0.49 \text{ mC/m}^2$, respectively. And the equivalent surface charge density σ was calculated according to equation (1)¹:

$$\sigma = \frac{\epsilon_r \epsilon_0 V}{d} \quad (1)$$

where σ is the surface charge density, V is the surface potential, ϵ_r and ϵ_0 are the relative permittivity of the electret film and the air, respectively. The measured surface potential was -2750 V , thus the equal surface charge density is approximately 0.49 mC m^{-2} .

A grounded air sphere with a diameter of 100 mm surrounded the entire setup. During the simulation, the dielectric permittivity ϵ were 1.0 for air and Cu film, 2.0 for PTFE, and 2.9 for the luminescent film. During the dynamic simulation, the probe position was set in the centre of the PTFE surface, and the Cu film moved in the same horizontal plane.

Characterization of the NCIVS.

The morphology of the NCIVS cross-section and surface morphology of the ZnS: Cu particles were characterised by field emission SEM at an accelerating voltage of 10 kV (Nova Nano 450, FEI, Japan). An X-ray diffractometer was used to record the X-ray diffraction (XRD) pattern (X'Pert3, PANalytical, Netherlands). Electrostatic Voltmeter was used to measure the surface potential of electret film (Monroe 279).

2. Supplementary figures

Control experiments to optimize the surface potential of the PTFE film by changing charge

voltages and mass ratio of PTFE NPs and ZCPs are shown in Fig. S1 and S2. As shown in Fig S1, the surface potential of the PTFE film grows with the increase of the needle voltage and reaches an approximate saturation value of -2750 V at the voltage of 7.0 kV. Meanwhile, as shown in Fig S2, the excess PTFE NPs results in particles aggregation, which in turn hampers the charge retention. As a result, the optimal experimental parameters were chosen as the voltage of 7.0 kV and mass ratio of 1:1 in this report.

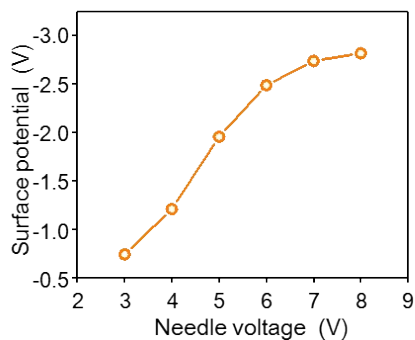


Figure S1. Surface potential of the NCIVS at different needle voltages during corona charging.

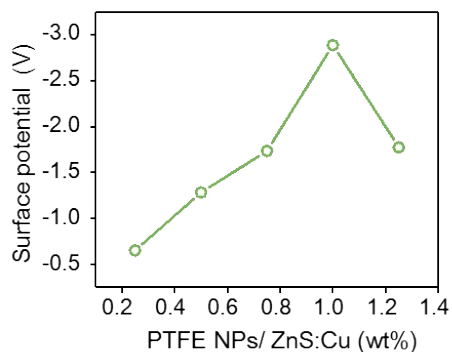


Figure S2. Surface potential of the NCIVS with different PTFE NPs/ ZnS: Cu particle mass ratios during corona charging.

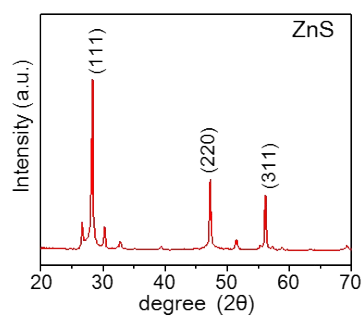


Figure S3. The X-ray diffraction (XRD) spectrometry of ZCPs. Three well-defined diffraction peaks corresponding to the lattice planes of (111), (220), and (311) are detected, which indicate the zinc-blended structure of ZnS.

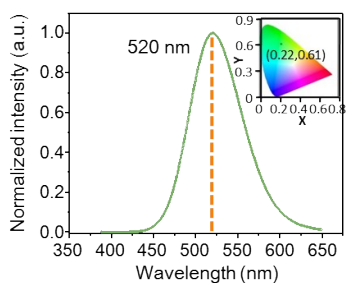


Figure S4. Wavelength spectrums of the NCIVS under UV light excitation and corresponding CIE coordinates.

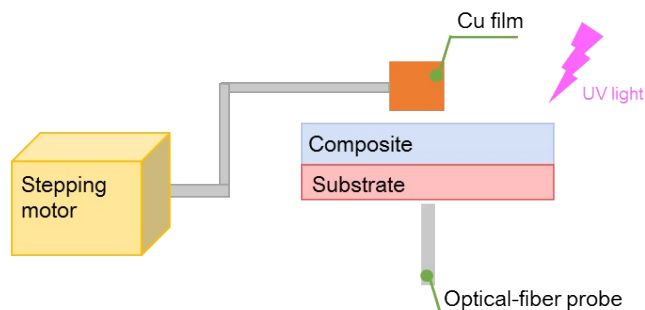


Figure S5. The test platform for measuring the luminescence intensity. The optic-fiber probe is close to the surface of the substrate, it could collect and transmit the emitted light to a spectrometer. The motion of the Cu film is driven by a linear stepper in a horizontal plane.

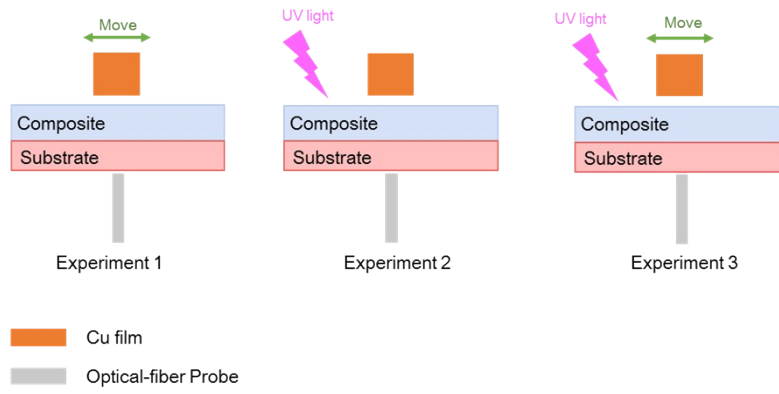


Figure S6. Three contrast experiments. Experiment 1: the Cu film is driven to move with the absence of UV excitation. Experiment 2: the Cu film is fixed under the UV excitation. Experiment 3: the Cu film is driven to move under the UV excitation.

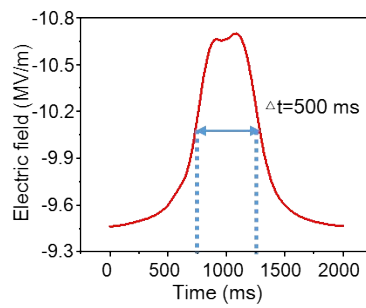


Figure S7. Electric field variation of the point P when the Cu film moves from position 1 to position 2.

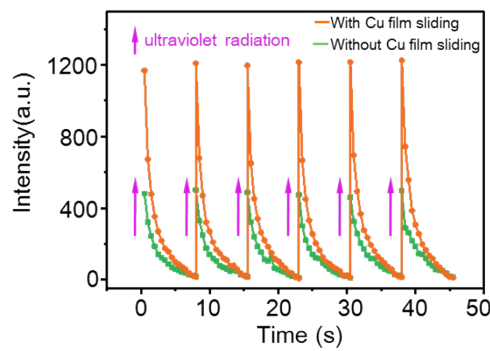


Figure S8. The luminescent intensity of the NCIVS under the pulsed UV excitation with the movable Cu film absent or present after several times of ultraviolet radiation. The emission intensity attenuates to zero within eight seconds regardless of the moving of Cu film.

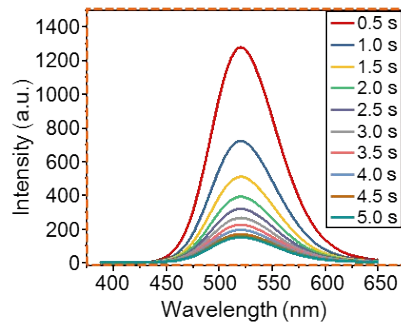


Figure S9. The specific spectrum of the NCIVS with the motion of Cu film, and the result indicates a fixed peak value at 520 nm.

The factors that influence the luminescence intensity were investigated in two aspects, i.e., the magnitude and the frequency of the AC-like electric field, as shown in Fig. S10. Firstly, the increasing surface potential of the PTFE film improves the luminescence intensity, as shown in Fig. S10a. The enhance factor, which defined as the emission intensity relative to the pure photon-excited intensity, is demonstrated in Fig. S10b. This can be explained by that the increscent AC-like electric field caused by the higher surface potential is more beneficial for lowering barrier height and enhancing emission intensity. Secondly, the distance between the NCIVS and the floating object is also related to the emission intensity, as shown in Fig. S10c, the relevant enhance factor is illustrated in Fig. S10d. The larger distance inevitably produces fewer induced-charges on the Cu film, leading to reduced amplitude of the AC-like electric field and emission intensity. Thirdly, as the moving velocity of Cu film becomes faster, the light emission would be stronger due to the acceleration of frequency, as shown in Fig. S10e and S10f. Finally, the emission intensity increases with the greater areas of the floating Cu film due to the larger bright zones, which is shown in Fig. S10g and S10h.

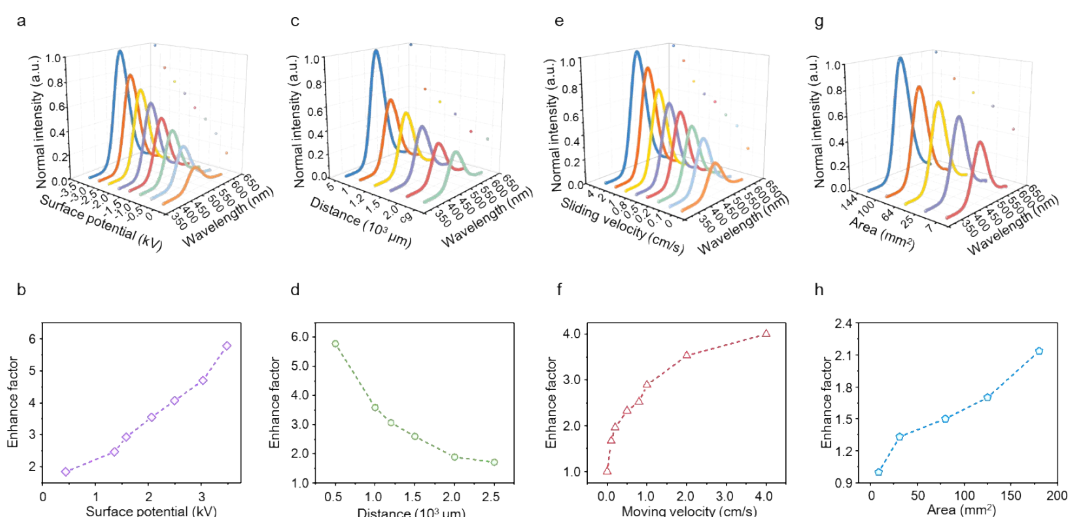


Figure S10. Factors influencing the luminescence intensity. (a-b) Relationship between the luminescence intensity, the enhanced factor with different surface potentials, (c-d) Relationship between the luminescence intensity, the enhanced factor with different separation distances, (e-f) Relationship between the luminescence intensity, the enhanced factor with different moving velocities of the Cu film, (g-h) Relationship between the luminescence intensity, the enhanced factor with different areas of the Cu film.

References

1. J. W. Zhong, Q. Z. Zhong, G. J. Chen, B. Hu, S. Zhao, X. Li, N. Wu, W. B. Li, H. M. Yu and J. Zhou, *Energy Environ. Sci*, 2016, 9, 3085-3091.